Global Journal of Engineering and Technology Advances
eISSN: 2582-5003
Cross Ref DOI: 10.30574/gjeta
Journal homepage: https://gjeta.com/

(RESEARCH ARTICLE)

Check for updates

Dynamic behavior of pin-free beam with torsional spring and hub at pinned end

Mohammed Taha Yassin * and Tahseen Taha Othman

Department of Mechanical Engineering, College of Engineering, Tikrit University, Iraq.

Global Journal of Engineering and Technology Advances, 2024, 18(02), 149–164

Publication history: Received on 29 December 2023; revised on 05 February 2024; accepted on 09 February 2024

Article DOI: https://doi.org/10.30574/gjeta.2024.18.2.0022

Abstract

This paper described the free vibration of a Euler-Bernoulli beam and discovered the first five dimensionless natural frequencies and mode shapes of motion for the pin-free beam model with a helical spring and rotating mass on the pinned side of the beam. The effect of changing the dimensionless torsional stiffness ratios was investigated, as was the effect of changing the dimensionless rotational inertia torque ratios Concerning the vibration properties of the beam. The mathematical equations that regulate the pin-free beam model were constructed using the exact analytical solution, establishing the Admissible Function and the natural frequency equation for the basic pin-free beam system. The approximate Rayleigh-Ritz approach was then used to determine the first five dimensionless natural frequencies, as well as the movement pattern for the pin-free beam model with a helical spring and a rotating mass on the side of the hinge. The results demonstrated that modifying the beam's natural frequencies is dependent on the ratios of the additional torsional spring parameters as well as the ratios rotational moment of inertia. The threshold system frequencies increase when the spring parameters are the major factor, and decrease when the inertia moment parameters are the main factor. Both play a role in influencing natural frequency to varied degrees. Unifying the final distribution of parameters might lead to optimizing the impact of parameters on the natural frequencies of the system.

Keywords: Pin-free beam; Free vibration; Helical spring; A Euler-Bernoulli beam; Rayleigh-Ritz method

1. Introduction

Because of the relevance of the beam in mechanical, civil, and aeronautical engineering applications, many researchers have expanded their interest in investigating the vibrational behavior of the beam in recent decades, as they play a key role in engineering structure applications. Structures' vibrations can be studied by representing them in the most basic manner imaginable, such as a beam. As a result, precisely establishing the natural frequencies and mode shape of these beams has become an essential topic Long and thin beams are created using Euler-Bernoulli beam theory or thin beam theory. Transverse vibrations or bending vibrations refer to the movement and vibration of a beam in a direction perpendicular to its length. Robot arms and weightlifts used in the construction of multi-story structures, among other applications, are two of the most important uses for beams. As beams bend and compress, vibration develops throughout their movement due to their flexibility. The beam stores potential energy from bending by virtue of its deflection and kinetic energy from the mass's moment of inertia around the longitudinal axis by virtue of its speed, If we assume that the beam is pin free beam, we will be able to study the effect of the torsional stiffens of the parts transmitting the movement between the beam and the motor, as well as study the effect of the moment of inertia of the center of the rotation axis the hup on the natural frequency and mode shapes of the beam.

The type of beam boundary conditions can play an essential role in how the beam responds. For example, torsional stiffness plays a role in raising the natural frequencies and its effect is evident at low frequencies, and its effect decreases at high frequencies, while inertial torque reduces the natural frequencies of the system. Its effect is more noticeable at high frequencies. In some studies, the system is considered to be a fixed free beam, which leads to not taking into account

* Corresponding author: Mohammed Taha Yassin

the effect of torsion stiffnesses on the beam frequency, and it is used because it can reduce the complexity of the solution. Which may lead to any prediction of dynamic response being inaccurate.

The phenomenon of adding flexible constraints to beams, and a large number of scientists have studied the natural properties of this type of beams from different points of view. Maurizi, Rossi et al (1)deal with the free vibration of a beam hinged at one end by a rotational spring and subjected to the restraining action of a translational spring at the other end. Laura, Grossi et al (2) deals with the exact solution of the transferee vibrations of a beam elastically restrained at one end and with a mass and spring at the other subjected to an axial force. Rao and Mirza (3) restrained Bernoulli-Euler beams with unsymmetrical translations and rotations at either end.to Exact frequency and normal mode shape expressions are derived in this note for general. Kim and Kim (4) present a method to find accurate vibration frequencies of beams with generally restricted boundary conditions using Fourier series. da Silva, do Nascimento et al (5) The analysis of vibrating beams with ends elastically restrained against rotation and translation or with ends carrying concentrated masses. Hong, Dodson et al (6) applies the Euler-Bernoulli beam theory to this test bed to develop analytical solutions of the system Transverse Vibration of Clamped-Pinned-Free Beam with Mass at Free End. Song, Dong et al (7) studied the transverse vibration of Euler Bernoulli beam with mass of ends and springs. AL ghoul, Cabezas et al (8) derive an expression to calculate the natural frequencies and plot the mode shapes of a simply-supported beam with an overhang with an end overhang point mass by using the Euler Bernoulli theory in the case of free transverse vibrations. Kudryavtsev, Malykhina et al (9) Considers the problem of estimating the first eigenfrequency and the first critical force of the beam using the so-called support coefficients. The support coefficients are calculated for a variety of support stiffness combinations.

The current study has four sections: introduction, methodology, results, and conclusions. The methodology section describes a typical analysis for investigating the transverse vibrations of a Euler-Bernoulli beam that is pinned on one side and free on the other. The partial differential problem, admissible function, and frequency equation for the pin-free beam were all solved using the precise analytical solution approach. A helical spring and a rotating mass were then added on the pinned side of the beam, and the Rayleigh-Ritz method was used to find the natural frequencies and mode shapes of the corresponding to each frequency for different stiffness ratios and rotational inertia moment ratios. The results section and the article end with the conclusions.

2. Mathematical procedure

2.1. Beam pinned at left end and free at right end

Determining the Eigenvalue and Admissible Function The system is a Euler-Bernoulli type pinned-free beam. As seen in Figure (1), it is a pinned beam at x=0 and free at x=L. In it is assumed that the beam is uniform, made of homogeneous material, and vibrations in the horizontal plane.

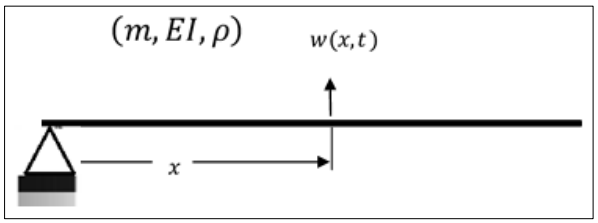

Figure 1 Structural simple system analysis

The partial differential equation governing the Euler-Bernoulli beam and the exact solution are applied to the uniform Bernoulli-Euler beam to determine the free vibration of the beam

$$EI(x)\ \frac{\partial^4 w(x,t)}{\partial x^4} + \rho A \frac{\partial^2 w(x,t)}{\partial t^2} = 0 \qquad 0 < x < L \qquad \cdots\cdots 1$$

where w is the lateral deflection, EI is the modulus of flexural rigidity of the beam, ρ is its density per unit volume, A is its cross-sectional area, x is the distance along measured from the beam end and t is the time.

To obtain the solution of the beam's free vibration, one uses the method of separation of variables and assumes a solution of form 2.

$$w(x,t) = W(x) * T(t) \qquad \cdots\cdots\cdots 2$$

$w(x,t)$ represents the product of two functions: the displacement function (W(x)) and the time function (T(t)), and its differentiation four times with respect to displacement (x) and twice with respect to time (t).

Equation 3 represents the general solution of the free transverse vibration equation for a uniform beam

$$W(x) = C_1 \cos\beta x + C_2 \sin\beta x + C_3 \cosh\beta x + C_4 \sinh\beta x \quad \cdots\cdots\cdots 3$$

The values of three constants may be discovered by substituting the four boundary conditions on both sides of the beam, since $C_1, C_2, C_3 and\ C_4$ are constants. The value of the fourth constant can be found by solving the two initial conditions.

$$\beta^4 = \frac{\rho A \omega^2}{EI} \qquad \cdots\cdots\cdots 4$$

The boundary conditions of a pin-free beam type, as illustrated in Figure 1, are deflection, bending moment, and shear force.

$$W(x)|_{x=0} = 0 \qquad \text{(deflection)} \qquad \cdots\cdots\cdots 5$$

$$\left.\frac{dW^2(x)}{dx^2}\right|_{x=0} = 0 \qquad \text{(bending moment)} \qquad \cdots\cdots 6$$

$$\left.\frac{dW^2(x)}{dx^2}\right|_{x=L} = 0 \qquad \text{(bending moment)} \qquad \cdots\cdots\cdots 7$$

$$\left.\frac{dW^3(x)}{dx^3}\right|_{x=L} = 0 \qquad \text{(shear force)} \qquad \cdots\cdots 8$$

Equation 9 was generated by applying the boundary condition to Equation 3. This equation represents the accepted function or the mode shapes equation for the pin-free beam system.

$$W(x) = \emptyset(x) = C_2 \left(\sin\beta x + \frac{\sin\beta L}{\sinh\beta L}\sinh\beta x\right) \qquad \cdots\cdots 9$$

where

$\emptyset(x)$: denotes the Eigen Function or the admissible function, for pin-free beam.

Equation 10 now represents the pin-free beam system's natural frequency equation

$$\tan\beta L - \tanh\beta L = 0 \qquad \cdots\cdots 10$$

2.2. pinned-free beam with connected to a torsional spring and point mass at left end and free at right end

The system consists of a pin free beam with a helical spring at the pin's end and a mass moment of inertia. Similar to Figure 2, employ the Rayleigh-Ritz approximation to determine the beams' vibrational characteristics by approximate analytical methods.

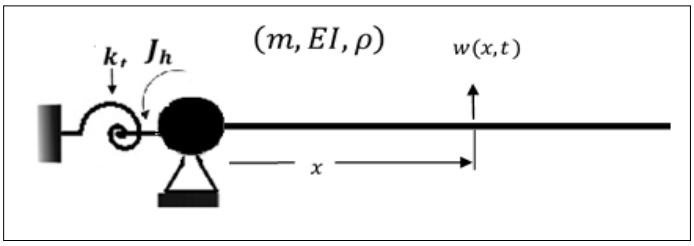

Figure 2 Structural system analysis

To obtain approximate eigenfunctions, the conservative distributed parameter system is approximated by a discrete model. The first step in the Rayleigh-Ritz method is to establish a minimization sequence, which imposes the form of equation 11.

$$Y^{(n)}(x) = \sum_{i=1}^{n} a_i \emptyset_i(x) \qquad \cdots\cdots 11$$

where

$\emptyset_i = \emptyset_1, \emptyset_2, \cdots, \emptyset_n(x)$ They represent independent empirical functions.

$a_i = a_1, a_2, \cdots, a_n$ symbolizes unidentified transactions.

The preferred form for the Rayleigh quotient is the energy form, that is, in which the numerator (N) is a measure of potential energy and the denominator (D) is a measure of kinetic energy, and the Rayleigh-Ritz quotient is a function of indefinite coefficients, so it is appropriate to write it in a form that can express the quotient of the Rayleigh method in general.

$$R(a_1, a_2, \cdots, a_n) = \frac{N(a_1, a_2, \cdots, a_n)}{D(a_1, a_2, \cdots, a_n)} \qquad \cdots\cdots 12$$

$$N = V_{max} = \frac{1}{2}\int_0^L EI(x) \sum_{i=1}^{n} a_i \frac{d^2\emptyset_i(x)}{dx^2} \sum_{j=1}^{n} a_j \frac{d^2\emptyset_j(x)}{dx^2} dx + k_t \sum_{i=1}^{n} a_i \frac{d\emptyset_i(0)}{dx} \sum_{j=1}^{n} a_j \frac{d\emptyset_j(0)}{dx}$$

$$= \frac{1}{2}\sum_{i=1}^{n}\sum_{j=1}^{n} a_i\, a_j \left[\int_0^L EI(x) \frac{d^2\emptyset_i(x)}{dx^2}\ \frac{d^2\emptyset_j(x)}{dx^2}\ dx + \ k_t\ \frac{d\emptyset_i(0)}{dx}\ \frac{d\emptyset_j(0)}{dx}\ \right]$$

$$= \frac{1}{2}\sum_{i=1}^{n}\sum_{j=1}^{n} a_i\, a_j\, k_{ij} \qquad \cdots\cdots 13$$

$$D = T^* = \frac{1}{2}\int_0^L \rho A \sum_{i=1}^{n} a_i\, \emptyset_i(x) \sum_{j=1}^{n} a_j\, \emptyset_j(x)\, dx + J_h \sum_{i=1}^{n} a_i \frac{d\emptyset_i(0)}{dx} \sum_{j=1}^{n} a_j \frac{d\emptyset_j(0)}{dx}$$

$$= \frac{1}{2}\sum_{i=1}^{n}\sum_{j=1}^{n} a_i\, a_j \left[\int_0^L \rho A\, \emptyset_i(x)\, \emptyset_j(x)\, dx + J_h\ \frac{d\emptyset_i(0)}{dx}\ \frac{d\emptyset_j(0)}{dx}\right]$$

$$= \frac{1}{2}\sum_{i=1}^{n}\sum_{j=1}^{n} a_i a_j\, m_{ij} \qquad \cdots\cdots 14$$

where

V_{max} It is the maximum stress energy or potential energy where.

T^*_{max} Represents the reference kinetic energy.

k_t Represents the torsional stiffness of the helical spring.

J_h The rotational moment of inertia of the hub rotation.

K=k_{ij} Stiffness matrix

M=m_{ij} mass matrix

As shown below, if variations of the indefinite coefficients (a_i) are performed, we obtain the equation *15*.

$$\frac{\partial N}{\partial \vec{a}} - \lambda^{(n)} \frac{\partial D}{\partial \vec{a}} = 0 \qquad \cdots\cdots 15$$

Equation 15 is a system of algebraic homogeneous linear equations that represents the requirements required for the stability of the Rayleigh-Ritz quotient. Since the eigenvalue is represented by $\lambda^{(n)}$ and the superscript n indicates that the eigenvalue problem corresponds to a series of n terms in equation 15,

Equations 13 and 14 were substituted into equation 15 to carry out variations for the indeterminate coefficients (a_i). The following equations are obtained.

$$\frac{\partial N}{\partial \vec{a}} = \frac{1}{2}\sum_{i=1}^{n} a_i\, k_{ij} \qquad \cdots\cdots\cdots 16$$

$$\frac{\partial D}{\partial \vec{a}} = \frac{1}{2}\sum_{i=1}^{n} a_i\, m_{ij} \qquad \cdots\cdots\cdots 17$$

$$\frac{1}{2}\sum_{i=1}^{n} a_i\, k_{ij} - \lambda^{(n)}\frac{1}{2}\sum_{i=1}^{n} a_i\, m_{ij} = 0 \quad , i = 1,2,\cdots,n \qquad \cdots\cdots 18$$

$$K^n a^n = \lambda^n M^n a^n \qquad \ldots\ldots 19$$

$$\omega^2 = \lambda = \frac{\sum_{i=1}^{n}\sum_{j=1}^{n} a_i \left[\int_0^L EI(x)\frac{d^2\emptyset_i(x)}{dx^2}\ \frac{d^2\emptyset_j(x)}{dx^2}\ dx + \ \alpha_1\ \frac{d\emptyset_i(0)}{dx}\ \frac{d\emptyset_j(0)}{dx}\ \right]}{\sum_{i=1}^{n}\sum_{j=1}^{n} a_i \left[\int_0^L \rho A\, \emptyset_i(x)\, \emptyset_j(x)\, dx + \alpha_2\ \frac{d\emptyset_i(0)}{dx}\ \frac{d\emptyset_j(0)}{dx}\right]} \ldots\ldots 20$$

$$Y^i(X) = \sum_{j=1}^{n} a_j^{(i)}\, \emptyset_j(x) = \ a_1^{(i)}\, \emptyset_1(x) + a_2^{(i)}\emptyset_2(x) + \cdots + a_n^{(i)}\emptyset_n(x) \qquad \ldots\ldots 21$$

Equations 19 indicate the solution of the algebraic eigenvalue problem of order n. To obtain a non-trivial solution of the vector ($\vec{a}$), the determinant of the coefficient's matrix must equal zero. For each natural frequency ω_i, the corresponding vector of Ritz coefficients ($a_n^{(i)}$) within an arbitrary constant can be determined by solving the simultaneous linear homogeneous equations.

Equation 22 indicates the natural frequency

$$\omega_i = \sqrt{\lambda} = (\beta_i l)^2 \sqrt{\frac{EI}{\rho A l^4}} \qquad \ldots\ldots\ 22$$

The torsional stiffness of the helical spring (k_t) and the stiffness of the beam in equation 23. expressed as a ratio, are represented by the dimensionless torsional stiffness values (α_1).

$$\alpha_1 = \frac{k_t}{(EI/L)forbeam} \qquad \ldots\ldots.23$$

Finding the values of the dimensionless rotational inertia moment (α_2) in equation 24, which is a ratio between the torque of the beam mass around the rotation axis and the rotational inertia moment of the hup around the vibration axis.

$$\alpha_2 = \frac{J_h}{(m(x)L^3)forbeam} \qquad \ldots\ldots.24$$

3. Results

For the Euler-Bernoulli beam model, which is pinned on one side and free on the other as shown in Figure (1), find the dimensionless natural frequencies (β_n l) as shown in Table (1). Similarly, find the mode shapes corresponding to each frequency as shown in Figure (3), since the value is from ($\alpha_1 = 0$) and ($\alpha_2 = 0$).

Table 1 Results for the natural frequencies of the pin-free beam system

natural frequencies	$(\beta_1 l)$	$(\beta_2 l)$	$(\beta_3 l)$	$(\beta_4 l)$	$(\beta_5 l)$
	0	3.926602	7.068582	10.21017	13.351768

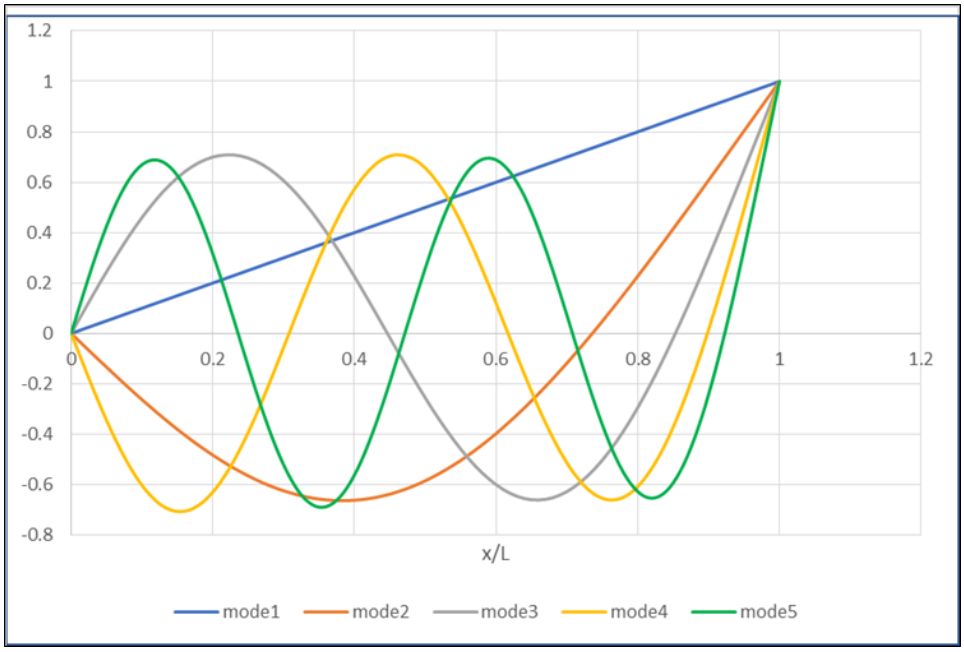

Figure 3 The five movement patterns of the pin-free beam system

The pin-free beam's vibrating behavior, which is aided by a helical spring on its pinned side. The dimensionless torsional spring values (α_1) were used in the range (0,1, 2, 6, 10, 16, 20, and 24) to show the impact of adding the helical spring on the values of the natural frequencies and the mode shape. The value of (α_2) was assumed to be zero.

Table 2 The increase in the amount of dimensionless frequencies as a result of increasing torsional rigidity $(\boldsymbol{\alpha_1})$

$\boldsymbol{\alpha_1 = \frac{k_t}{E_b I_b / L_b}}$	$\boldsymbol{\alpha_1 = 0}$	$\boldsymbol{\alpha_1 = 1}$	$\boldsymbol{\alpha_1 = 2}$	$\boldsymbol{\alpha_1 = 6}$	$\boldsymbol{\alpha_1 = 10}$	$\boldsymbol{\alpha_1 = 16}$	$\boldsymbol{\alpha_1 = 20}$	$\boldsymbol{\alpha_1 = 24}$
$(\beta_1 l)$	0.0000	1.2589	1.4411	1.6939	1.7801	1.8393	1.8613	1.8767
$(\beta_2 l)$	3.9266	4.0351	4.1240	4.3591	4.4927	4.6104	4.6608	4.6985
$(\beta_3 l)$	7.0686	7.1368	7.2000	7.4087	7.5625	7.7254	7.8042	7.8669
$(\beta_4 l)$	10.210	10.258	10.306	10.484	10.641	10.838	10.946	11.037
$(\beta_5 l)$	13.351	13.389	13.428	13.589	13.759	14.026	14.209	14.394

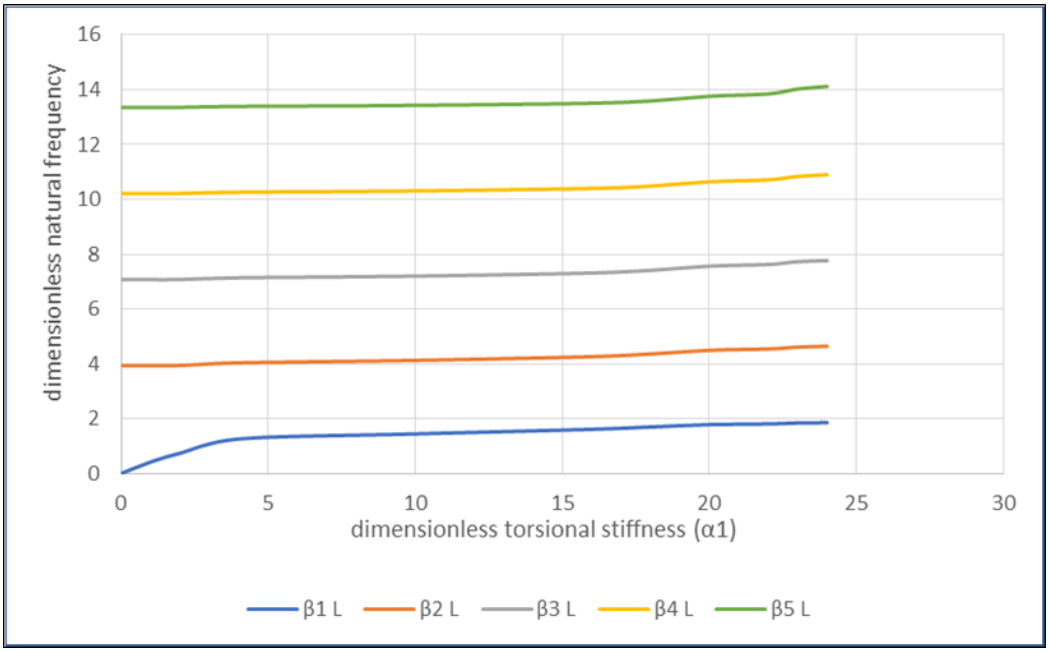

Figure 4 The increase in the natural frequency as a result of the increase in torsional stiffness $(\boldsymbol{\alpha_1})$

Table (2) shows the first five dimensionless frequencies and shows the increase in the amount of all-natural dimensionless frequencies as a result of the effect of the torsional spring, and its effect is more pronounced at low frequencies. It is also observed that when the torsional stiffness (α_1) becomes equal to (0), the system becomes a beam free of the pin. When the torsional stiffness (α_1) increases to (24), the system turns into a free fixed beam. As the graph in Figure (4) shows, the dimensionless natural frequencies rise ($\beta_n l$) as a result of the increase in the dimensionless torsional spring (α_1).

A rotating mass on one side pinned to the beam and the other end free supports the pin-free beam's vibrational behavior. To clarify the impact of the hup's moment of inertia on the natural frequencies and patterns of movement, the values of the dimensionless inertia moment (α_2) in the following ranges were used: (2×10^(-3), 4×10^(-3), 8×10^(-3), 2×10^(-2), 4×10^(-2), 7×10^(-2) and 9×10^(-2))) and the value of (α_1) was forced to equal zero.

Table 3 The effect of the dimensionless rotational moment of inertia ($\boldsymbol{\alpha_2}$) on the natural frequencies ($\boldsymbol{\beta_n l}$).

$\alpha_2 = \frac{J_h}{m(x)L^3}$	$\alpha_2 = 0$	$\alpha_2 =$ **0.0002**	$\alpha_2 =$ **0.0004**	$\alpha_2 =$ **0.0008**	$\alpha_2 =$ **0.002**	$\alpha_2 =$ **0.004**	$\alpha_2 =$ **0.007**	$\alpha_2 =$ **0.009**
$(\beta_1 l)$	0.0000	0.0000	0.0000	0.0000	0.0000	0.0000	0.0000	0.0000
$(\beta_2 l)$	3.9266	3.9209	3.9152	3.9038	3.8698	3.8144	3.7347	3.6842
$(\beta_3 l)$	7.0686	7.0332	6.9980	6.9285	6.7307	6.4508	6.1418	5.9910
$(\beta_4 l)$	10.2102	10.1063	10.0081	9.8302	9.4351	9.0735	8.8232	8.7340
$(\beta_5 l)$	13.3518	13.1428	12.9801	12.7465	12.3965	12.1847	12.0695	12.0321

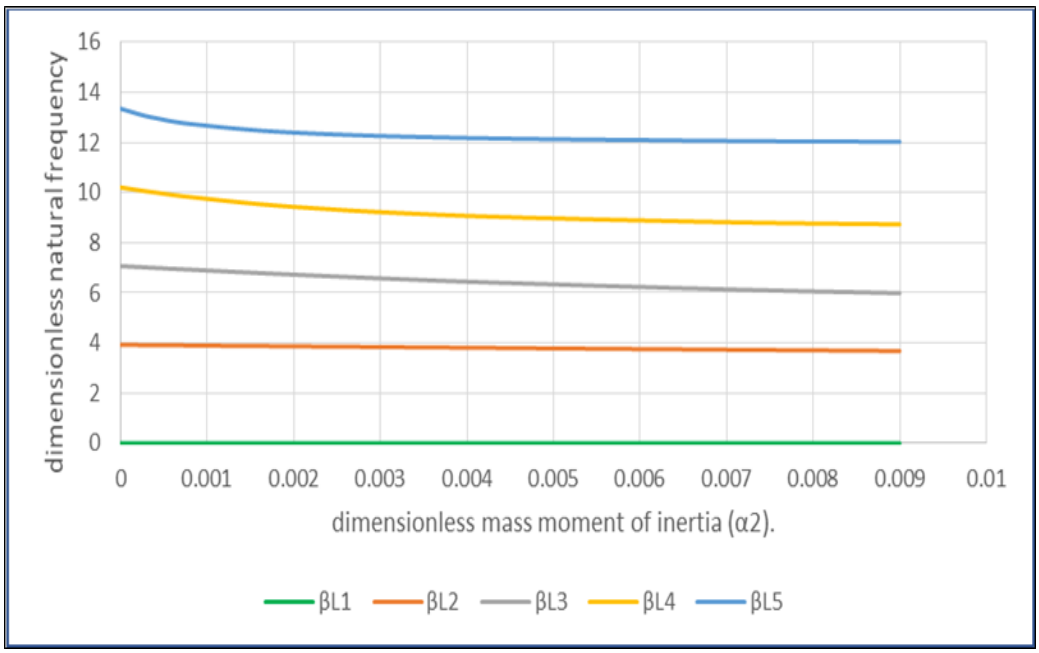

Figure 5 A schematic diagram showing the effect of increasing the dimensionless rotational moment of inertia on the natural frequency values

Table (3) illustrates the first five dimensionless natural frequencies as well as how the rotational mass moment of inertia causes all dimensionless natural frequencies to decrease in magnitude. The moment of inertia has a less impact at low frequencies and a larger influence at high frequencies. The dimensionless natural frequencies ($\beta_n l$) drop as the dimensionless mass moment of inertia (α_2) increases, as the graph in Figure (5) illustrates.

A study of the impact of torsional stiffness and rotational moment of inertia on the natural frequency and mode shape of the beam system presented in Figure (2), which illustrates the vibration behavior of the beam supported by a helical spring and a rotating mass at the pinned end and the other end is free.

As shown in Tables (4), (5), (6), (7) and (8), which show tables for the first five natural frequencies, respectively, and show that the natural frequencies of the beam are affected as a result of adding the rotating mass and the helical spring. The tables show the rate of frequency change. The symbol (↑) indicates an increase in frequencies, while the symbol (↓) indicates a decrease in frequencies. The three-dimensional diagrams accompanying each frequency are shown in the following figures (6), (7), (8), (9) and (10) which explains the effect of the values of torsional spring (α_1) and rotational moment of inertia (α_2) together on the dimensionless natural frequency.

Table 4 The effect of both torsional stiffness ($\boldsymbol{\alpha_1}$) and rotational moment of inertia ($\boldsymbol{\alpha_2}$) together on the specific value of the first natural frequency ($\boldsymbol{\beta L_1}$)

$\boldsymbol{\beta L_1}$	$\boldsymbol{\alpha_2 =}$ **0**	$\boldsymbol{\alpha_2 =}$ **0.0002**	$\boldsymbol{\alpha_2 =}$ **0.0004**	$\boldsymbol{\alpha_2 =}$ **0.0008**	$\boldsymbol{\alpha_2 =}$ **0.002**	$\boldsymbol{\alpha_2 =}$ **0.004**	$\boldsymbol{\alpha_2 =}$ **0.007**	$\boldsymbol{\alpha_2 =}$ **0.009**
$\alpha_1 = 0$	0.0000	0.0000	0.0000	0.0000	0.0000	0.0000	0.0000	0.0000
$\alpha_1 = 1$	1.2589	1.2587	1.2586	1.2583	1.2575	1.2562	1.2543	1.2530
$\alpha_1 = 2$	1.4411	1.4410	1.4409	1.4407	1.4400	1.4389	1.4372	1.4361
$\alpha_1 = 4$	1.6097	1.6096	1.6095	1.6094	1.6089	1.6082	1.6070	1.6063
$\alpha_1 = 6$	1.6939	1.6938	1.6938	1.6937	1.6934	1.6928	1.6920	1.6915
$\alpha_1 = 10$	1.7801	1.7801	1.7800	1.7800	1.7798	1.7795	1.7791	1.7788
$\alpha_1 = 12$	1.8053	1.8052	1.8052	1.8052	1.8050	1.8048	1.8045	1.8042
$\alpha_1 = 16$	1.8393	1.8393	1.8393	1.8393	1.8392	1.8390	1.8388	1.8386
$\alpha_1 = 18$	1.8514	1.8514	1.8514	1.8514	1.8513	1.8511	1.8510	1.8508
$\alpha_1 = 20$	1.8613	1.8613	1.8613	1.8613	1.8612	1.8611	1.8610	1.8608
$\alpha_1 = 22$	1.8696	1.8696	1.8696	1.8696	1.8696	1.8695	1.8693	1.8692
$\alpha_1 = 24$	1.8767	1.8767	1.8767	1.8767	1.8766	1.8766	1.8764	1.8764

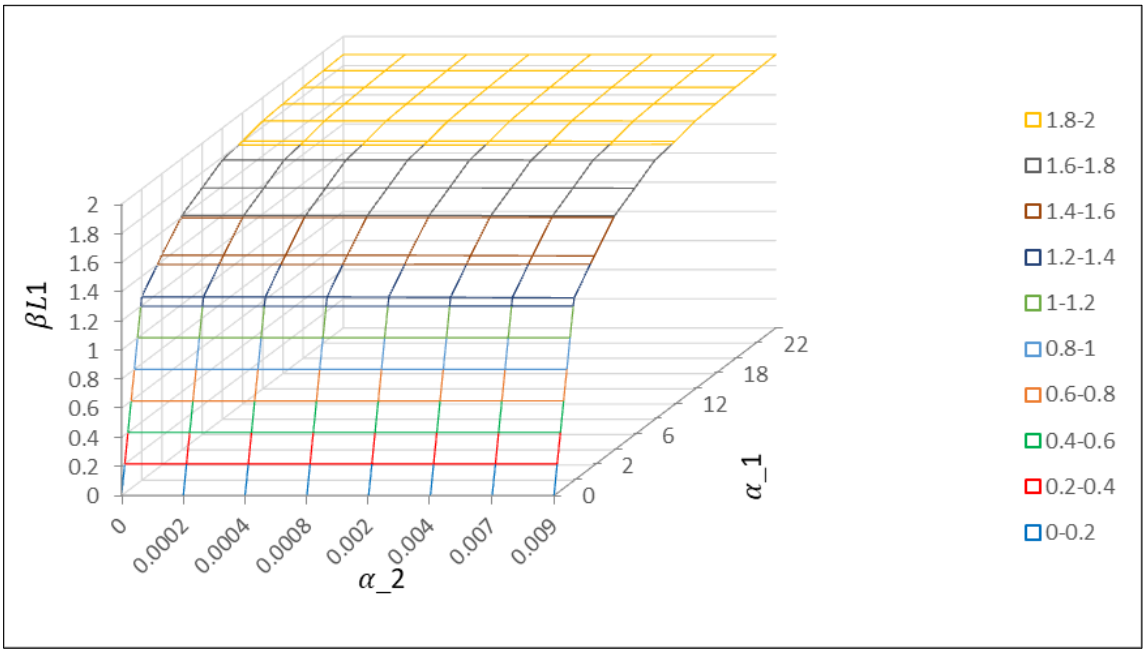

Figure 6 The effect of the ratios of both the torsional spring ($\boldsymbol{\alpha_1}$) and the rotational inertia moment ($\boldsymbol{\alpha_2}$) together on the first natural frequency ($\boldsymbol{\beta L_1}$)

Table 5 Effect of both torsional stiffness ($\boldsymbol{\alpha_1}$) and rotational moment of inertia ($\boldsymbol{\alpha_2}$) together on the specific value of the second natural frequency ($\boldsymbol{\beta L_2}$)

$\boldsymbol{\beta L_2}$	$\boldsymbol{\alpha_2 =}$ **0**	$\boldsymbol{\alpha_2 =}$ **0.0002**	$\boldsymbol{\alpha_2 =}$ **0.0004**	$\boldsymbol{\alpha_2 =}$ **0.0008**	$\boldsymbol{\alpha_2 =}$ **0.002**	$\boldsymbol{\alpha_2 =}$ **0.004**	$\boldsymbol{\alpha_2 =}$ **0.007**	$\boldsymbol{\alpha_2 =}$ **0.009**
$\alpha_1 = 0$	3.9266	3.9209↓	3.9152↓	3.9038↓	3.8698↓	3.8144↓	3.7347↓	3.6842↓
$\alpha_1 = 1$	4.0351↑	4.0300↑	4.0248↑	4.0144↑	3.9833↑	3.9319↓	3.8564↓	3.8078↓
$\alpha_1 = 2$	4.1240↑	4.1193↑	4.1146↑	4.1053↑	4.0770↑	4.0298↑	3.9593↑	3.9132↓
$\alpha_1 = 4$	4.2601↑	4.2563↑	4.2525↑	4.2449↑	4.2217↑	4.1824	4.1223↑	4.0818↑
$\alpha_1 = 6$	4.3591↑	4.3560↑	4.3529↑	4.3467↑	4.3276↑	4.2950↑	4.2442↑	4.2094↑
$\alpha_1 = 10$	4.4927↑	4.4906↑	4.4884↑	4.4841↑	4.4709↑	4.4480↑	4.4117↑	4.3864↑
$\alpha_1 = 12$	4.5398↑	4.5380↑	4.5361↑	4.5325↑	4.5213↑	4.5019↑	4.4710↑	4.4492↑
$\alpha_1 = 16$	4.6104↑	4.6091↑	4.6077↑	4.6050↑	4.5967↑	4.5824↑	4.5595↑	4.5432↑
$\alpha_1 = 18$	4.6375↑	4.6364↑	4.6352↑	4.6329↑	4.6257↑	4.6131↑	4.5932↑	4.5790↑
$\alpha_1 = 20$	4.6608↑	4.6598↑	4.6588↑	4.6567↑	4.6504↑	4.6394↑	4.6219↑	4.6095↑
$\alpha_1 = 22$	4.6809↑	4.6800↑	4.6791↑	4.6773↑	4.6717↑	4.6620↑	4.6465↑	4.6356↑
$\alpha_1 = 24$	4.6985↑	4.6977↑	4.6969↑	4.6953↑	4.6903↑	4.6817↑	4.6679↑	4.6582↑

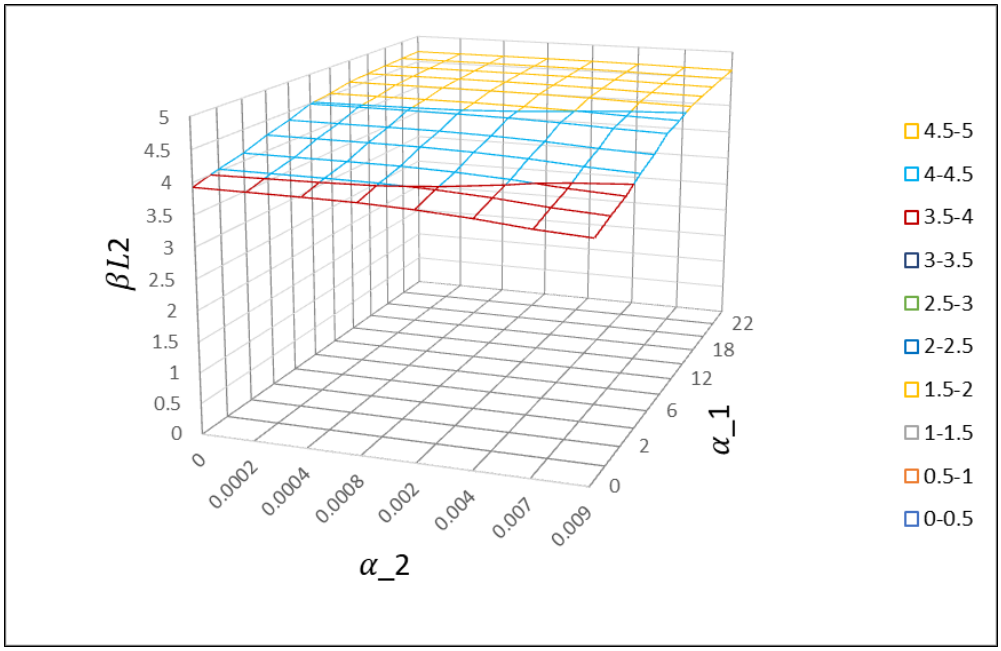

Figure 7 The effect of the ratios of both the torsional spring ($\boldsymbol{\alpha_1}$) and the rotational inertia moment ($\boldsymbol{\alpha_2}$) together on the second natural frequency ($\boldsymbol{\beta L_2}$).

Table 6 The effect of both torsional stiffness ($\boldsymbol{\alpha_1}$) and rotational moment of inertia ($\boldsymbol{\alpha_2}$) together on the specific value of the thread natural frequency ($\boldsymbol{\beta L_3}$)

$\boldsymbol{\beta L_3}$	$\boldsymbol{\alpha_2 =}$ **0**	$\boldsymbol{\alpha_2 =}$ **0.0002**	$\boldsymbol{\alpha_2 =}$ **0.0004**	$\boldsymbol{\alpha_2 =}$ **0.0008**	$\boldsymbol{\alpha_2 =}$ **0.002**	$\boldsymbol{\alpha_2 =}$ **0.004**	$\boldsymbol{\alpha_2 =}$ **0.007**	$\boldsymbol{\alpha_2 =}$ **0.009**
$\alpha_1 = 0$	7.0686	7.0332↓	6.9980↓	6.9285↓	6.7307↓	6.4508↓	6.1418↓	5.9910↓
$\alpha_1 = 1$	7.1368↑	7.1028↑	7.0687↑	7.0009↓	6.8052↓	6.5216↓	6.2016↓	6.0434↓
$\alpha_1 = 2$	7.2000↑	7.1673↑	7.1345↑	7.0688↑	6.8764↓	6.5909↓	6.2616↓	6.0965↓
$\alpha_1 = 4$	7.3125↑	7.2826↑	7.2524↑	7.1915↑	7.0082↓	6.7240↓	6.3807↓	6.2039↓
$\alpha_1 = 6$	7.4087↑	7.3816↑	7.3542↑	7.2983↑	7.1264↑	6.8484↓	6.4972↓	6.3111↓
$\alpha_1 = 10$	7.5625↑	7.5405↑	7.5181↑	7.4720↑	7.3249↑	7.0693↓	6.7171↓	6.5194↓
$\alpha_1 = 12$	7.6242↑	7.6045↑	7.5843↑	7.5425↑	7.4077↑	7.1660↑	6.8190↓	6.6186↓
$\alpha_1 = 16$	7.7254↑	7.7094↑	7.6929↑	7.6587↑	7.5461↑	7.3342↑	7.0056↓	6.8046↓
$\alpha_1 = 18$	7.7672↑	7.7527↑	7.7378↑	7.7067↑	7.6040↑	7.4069↑	7.0903↑	6.8912↓
$\alpha_1 = 20$	7.8042↑	7.7911↑	7.7775↑	7.7493↑	7.6556↑	7.4728↑	7.1694↑	6.9733↓
$\alpha_1 = 22$	7.8373↑	7.8253↑	7.8130↑	7.7873↑	7.7017↑	7.5325↑	7.2432↑	7.0510↓
$\alpha_1 = 24$	7.8669↑	7.8560↑	7.8448↑	7.8213↑	7.7430↑	7.5866↑	7.3120↑	7.1245↑

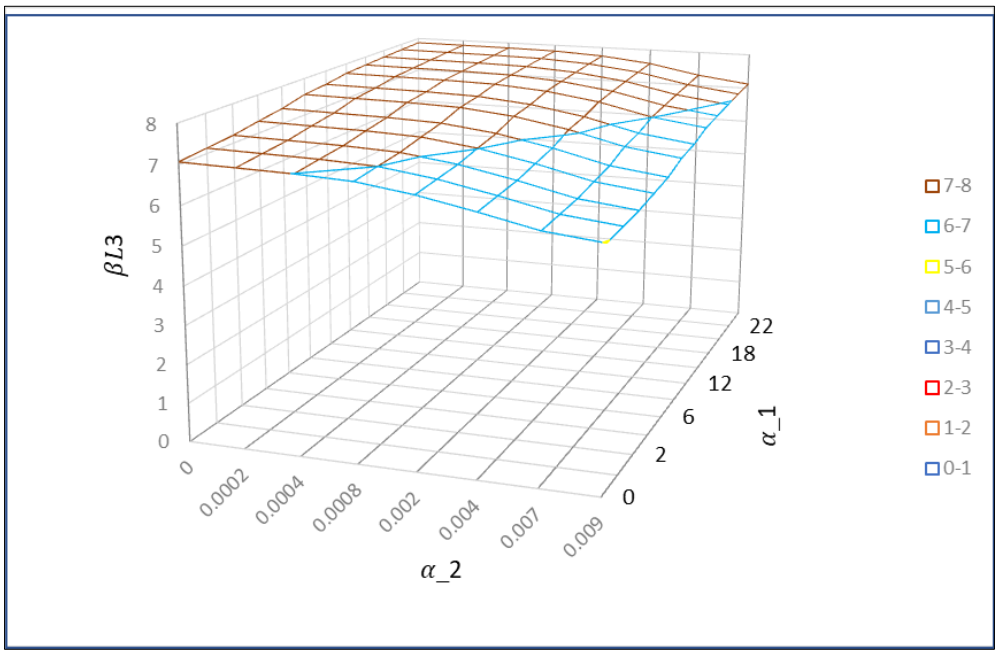

Figure 8 The effect of the ratios of both the torsional spring ($\boldsymbol{\alpha_1}$) and the rotational inertia moment ($\boldsymbol{\alpha_2}$) together on the thread natural frequency ($\boldsymbol{\beta L_3}$).

Table 7 The effect of both torsional stiffness ($\boldsymbol{\alpha_1}$) and rotational moment of inertia ($\boldsymbol{\alpha_2}$) together on the specific value of the fourth natural frequency ($\boldsymbol{\beta L_4}$)

$\boldsymbol{\beta L_4}$	$\boldsymbol{\alpha_2 =}$ **0**	$\boldsymbol{\alpha_2 =}$ **0.0002**	$\boldsymbol{\alpha_2 =}$ **0.0004**	$\boldsymbol{\alpha_2 =}$ **0.0008**	$\boldsymbol{\alpha_2 =}$ **0.002**	$\boldsymbol{\alpha_2 =}$ **0.004**	$\boldsymbol{\alpha_2 =}$ **0.007**	$\boldsymbol{\alpha_2 =}$ **0.009**
$\alpha_1 = 0$	10.2102	10.1063↓	10.0081↓	9.8302↓	9.4351↓	9.0735↓	8.8232↓	8.7340↓
$\alpha_1 = 1$	10.258↑	10.1545↓	10.0554↓	9.8745↓	9.4679↓	9.0922↓	8.8324↓	8.7403↓
$\alpha_1 = 2$	10.3061↑	10.2020↓	10.1023↓	9.9189↓	9.5013↓	9.1115↓	8.8419↓	8.7468↓
$\alpha_1 = 4$	10.3976↑	10.2945↑	10.1945↓	10.007↓	9.5699↓	9.1519↓	8.8618↓	8.7602↓
$\alpha_1 = 6$	10.4841↑	10.3831↑	10.2838↑	10.0951↓	9.6405↓	9.1946↓	8.8829↓	8.7744↓
$\alpha_1 = 10$	10.6414↑	10.5466↑	10.4513↑	10.2644	9.7858↓	9.2866↓	8.9289↓	8.8054↓
$\alpha_1 = 12$	10.7120↑	10.6212↑	10.5289↑	10.3450↑	9.8594↓	9.3356↓	8.9539↓	8.8221↓
$\alpha_1 = 16$	10.8382↑	10.7559↑	10.6707↑	10.4962↑	10.0062↓	9.4391↓	9.0082↓	8.8586↓
$\alpha_1 = 18$	10.8943↑	10.8164↑	10.7351↑	10.5665↑	10.0785↓	9.4931↓	9.0375↓	8.8783↓
$\alpha_1 = 20$	10.9460↑	10.8725↑	10.7953↑	10.6330↑	10.1497↓	9.5483↓	9.0682↓	8.8990↓
$\alpha_1 = 22$	10.9938↑	10.9246↑	10.8513↑	10.695↑	10.2193↑	9.6044↓	9.1003↓	8.9209↓
$\alpha_1 = 24$	11.0379↑	10.9728↑	10.9035↑	10.7551↑	10.2873↑	9.6612↓	9.1339↓	8.9438↓

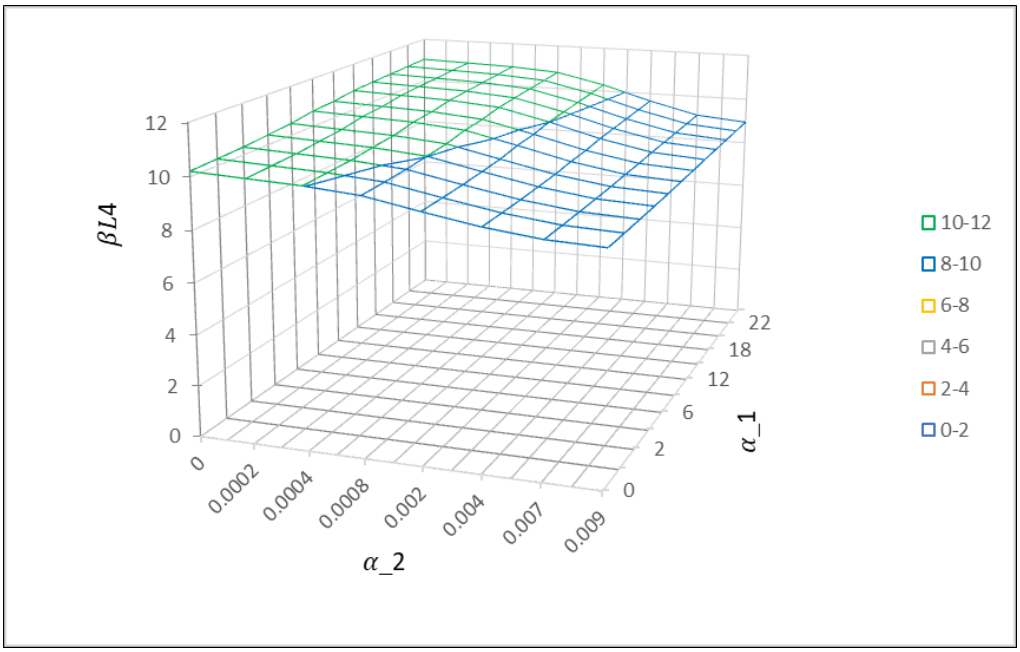

Figure 9 The effect of the ratios of both the torsional spring ($\boldsymbol{\alpha_1}$) and the rotational inertia moment ($\boldsymbol{\alpha_2}$) together on the fourth natural frequency ($\boldsymbol{\beta L_4}$)

Table 8 The effect of both torsional stiffness ($\boldsymbol{\alpha_1}$) and rotational moment of inertia ($\boldsymbol{\alpha_2}$) together on the specific value of the fifth natural frequency ($\boldsymbol{\beta L_5}$)

$\boldsymbol{\beta L_5}$	$\boldsymbol{\alpha_2 =}$ **0**	$\boldsymbol{\alpha_2 =}$ **0.0002**	$\boldsymbol{\alpha_2 =}$ **0.0004**	$\boldsymbol{\alpha_2 =}$ **0.0008**	$\boldsymbol{\alpha_2 =}$ **0.002**	$\boldsymbol{\alpha_2 =}$ **0.004**	$\boldsymbol{\alpha_2 =}$ **0.007**	$\boldsymbol{\alpha_2 =}$ **0.009**
$\alpha_1 = 0$	13.351	13.142↓	12.980↓	12.746↓	12.396↓	12.184↓	12.069↓	12.032↓
$\alpha_1 = 1$	13.389↑	13.173↓	13.005↓	12.764↓	12.404↓	12.187↓	12.070↓	12.032↓
$\alpha_1 = 2$	13.428↑	13.205↓	13.032↓	12.783↓	12.411↓	12.190↓	12.071↓	12.033↓
$\alpha_1 = 4$	13.507↑	13.271↓	13.086↓	12.821↓	12.428↓	12.196↓	12.074↓	12.035↓
$\alpha_1 = 6$	13.589↑	13.339↓	13.143↓	12.862↓	12.445↓	12.202↓	12.076↓	12.036↓
$\alpha_1 = 10$	13.759↑	13.482↓	13.264↓	12.949↓	12.481↓	12.215↓	12.081↓	12.039↓
$\alpha_1 = 12$	13.847↑	13.557↑	13.328↓	12.995↓	12.501↓	12.222↓	12.083↓	12.041↓
$\alpha_1 = 16$	14.026↑	13.712↑	13.462↑	13.093↓	12.542↓	12.237↓	12.089↓	12.044↓
$\alpha_1 = 18$	14.118↑	13.792↑	13.531↑	13.145↓	12.565↓	12.244↓	12.091↓	12.046↓
$\alpha_1 = 20$	14.209↑	13.873↑	13.601↑	13.199↓	12.588↓	12.252↓	12.094↓	12.047↓
$\alpha_1 = 22$	14.302↑	13.955↑	13.673↑	13.254↓	12.613↓	12.261↓	12.097↓	12.049↓
$\alpha_1 = 24$	14.394↑	14.037↑	13.746↑	13.310↓	12.638↓	12.269↓	12.101↓	12.051↓

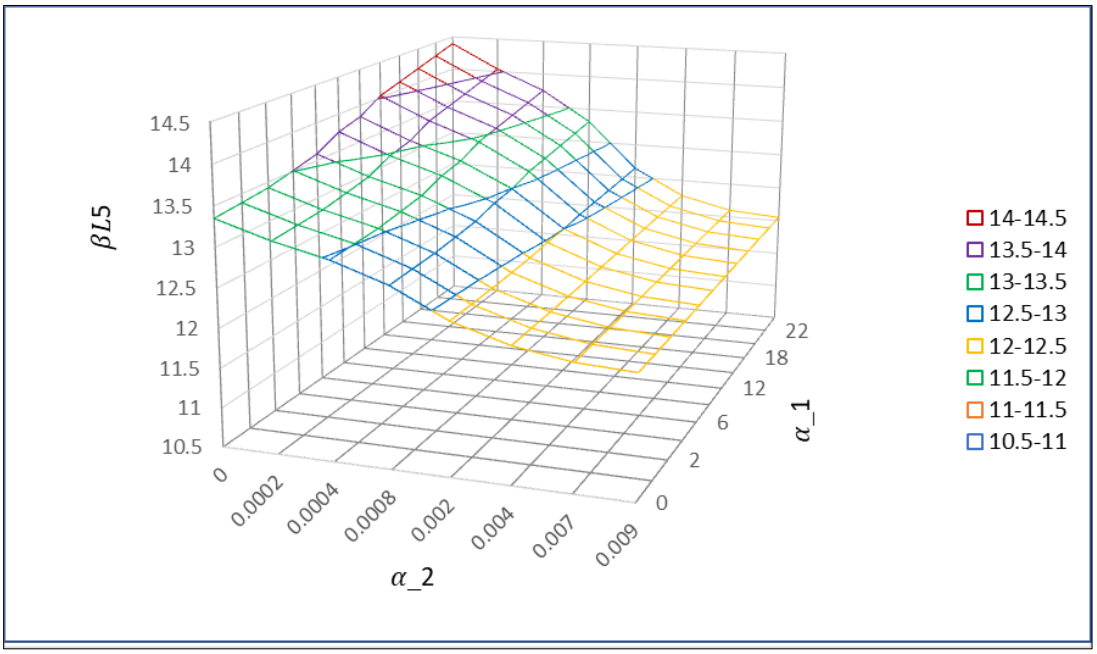

Figure 10 The effect of the ratios of both the torsional spring ($\boldsymbol{\alpha_1}$) and the rotational inertia moment ($\boldsymbol{\alpha_2}$) together on the fifth natural frequency ($\boldsymbol{\beta L_5}$).

Examining how torsional stiffness and rotational inertia torque affect the modes' shape in a beam system with a helical spring supporting it at one end and a spinning mass at the other, which is free, The second, third, and fourth forms of shape are depicted in Figures (11) (12) (13) (14) accordingly. These forms display movement patterns for various pinned beam support models and exhibit variance in the pattern vectors as a result of the impact of parameters on the rotational mass's moment of inertia and the beam's boundary conditions of spring stiffness.

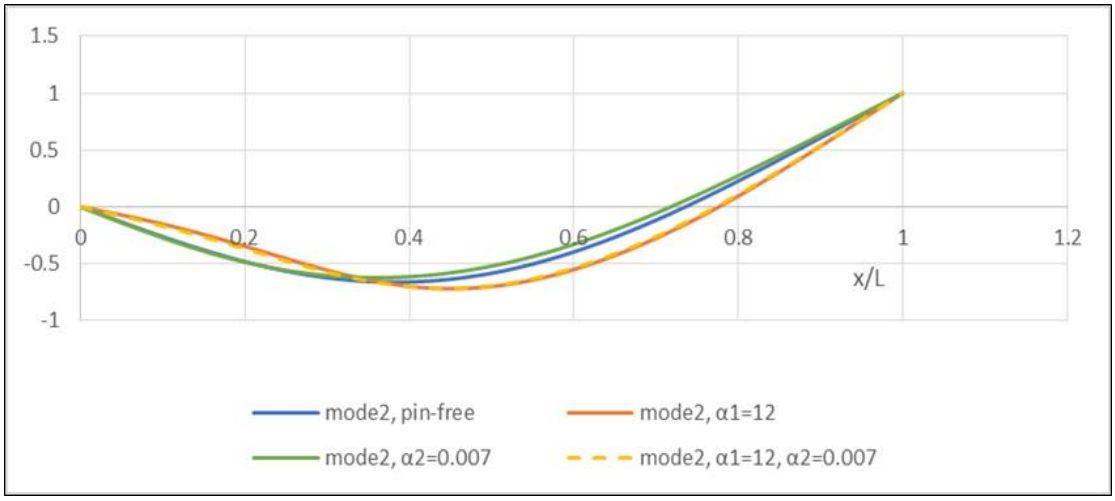

Figure 11 The second mode shape for several models of beam systems

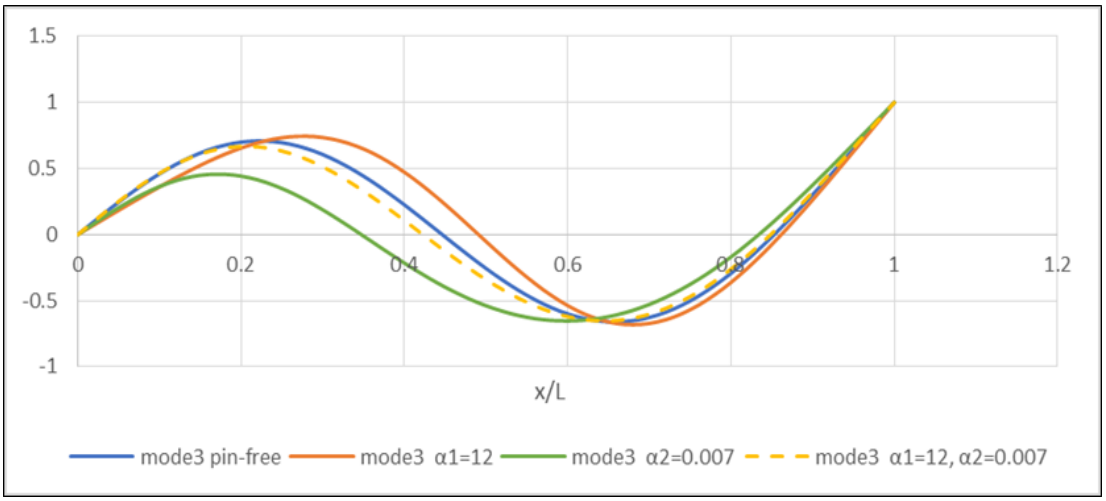

Figure 12 The third mode shape for several examples of beam systems

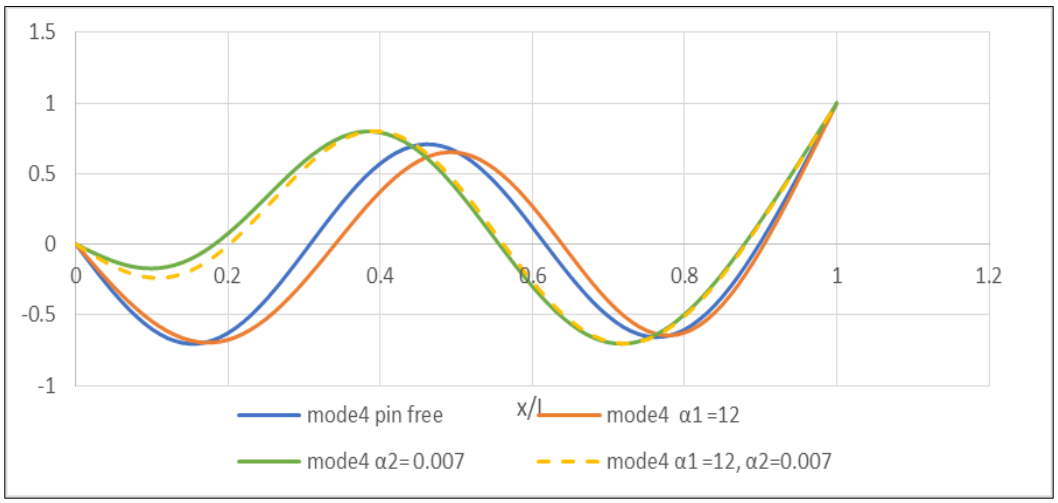

Figure 13 The fourth mode shape for several examples of beam systems

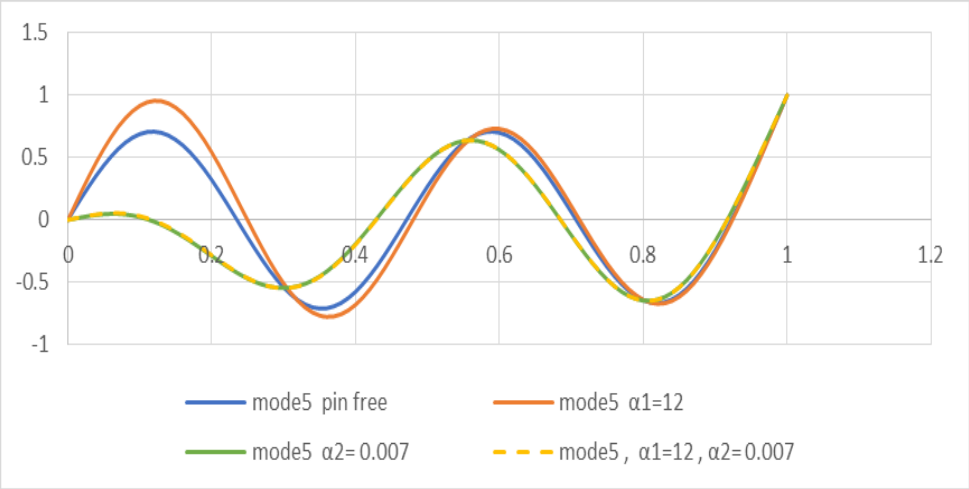

Figure 14 The fifth mode shape for several examples of beam systems

4. Conclusion

In this paper, the free vibration of the Euler-Bernoulli beam was analyzed for the pin-free beam system, which added to the helical spring mechanism and the rotating point mass on the pinned side of the threshold and free from the other end. First, the Eigen value and Eigen Function were obtained using the exact solution for the pin-free beam system. Then the approximate Rayleigh-Ritz method was used to study the effect of the ratios of the non-dimensional torsional spring parameters and the ratios of the rotational inertia moment parameters on the natural frequencies and mode shapes corresponding to the beam for the pin-free beam for system added to the helical spring mechanism and the rotating point mass on the pinned side. Following up on the results obtained Some conclusions are as follows

- Adding a helical spring at the end of the installed beam leads to an increase in the values of natural frequencies, and the reason is due to the increase in the equivalent stiffness of the beam system, as torsional stiffness has an effect on increasing of the values of natural frequencies and its effect is greater on the low frequencies and its effect decreases on the higher frequencies, Also, when the amount of torsional stiffness increases, the system will approach the free fixed beam system.
- Adding a helical spring increases the maximum bending amplitude of the mode shape.
- The addition of rotating mass at the fixed end of the beam leads to an increase in the mass matrix of the system, and the increase in the torque of rotational inertia leads to an increase in the kinetic energy of the system, which leads to a decrease in all natural frequencies of the system, and its effect is greater at higher frequencies, and the rate of change of frequency The beam is sharp at first, and as the amount of rotational inertia torque continues to increase, its effect on the natural frequency decreases while continuing to increase.
- Adding rotating mass leads to a decrease in the maximum amplitude of the curvature of the mode shape.
- The change of the natural frequencies of the beam depends on the ratios of the added parameters of the spring and the moment of inertia. If spring parameters are the main factor, the beam system frequencies rise. While if the moment of inertia parameters is the main factor, the beam system frequencies decrease, and standardizing the final distribution of parameters can improve the effect of the parameters on the natural frequencies of the system. The amount of torsional stiffness and the amount of rotational inertia moment must first be taken into account to create dynamic models with different required accuracy. The natural frequencies of the overall mechanical system must be predicted to avoid dangerous resonance.
- The type of beam boundary conditions determines the natural frequencies and the forms of the accompanying mode shape. A uniform distribution can also improve the mode shape, and modifying the final distribution can enhance the impact of boundary conditions on frequencies.

Compliance with ethical standards

Disclosure of Conflict of Interest

The author has no conflict of interest in this research.

References

[1] Maurizi M, Rossi R, Reyes J. Vibration frequencies for a uniform beam with one end spring-hinged and subjected to a translational restraint at the other end. Journal of Sound and Vibration. 1976;48(4):565-8.

[2] Laura PA, Grossi RO, Alvarez S. Transverse vibrations of a beam elastically restrained at one end and with a mass and spring at the other subjected to an axial force. Nuclear Engineering and Design. 1983;74(2):299-302.

[3] Rao CK, Mirza S. A note on vibrations of generally restrained beams. Journal of Sound and Vibration. 1989;130(3):453-65.

[4] Kim H, Kim M. Vibration of beams with generally restrained boundary conditions using Fourier series. Journal of Sound and Vibration. 2001;245(5):771-84.

[5] da Silva JF, do Nascimento LAD, dos Santos Hoefel S, editors. Free vibration analysis of Euler-Bernoulli beams under non-classical boundary conditions. IX Congresso Nacional de Engenharia Mecânica CONEM2016, Fortaleza-CE, Brasil; 2016.

[6] Hong J, Dodson J, Laflamme S, Downey A. Transverse vibration of clamped-pinned-free beam with mass at free end. Applied Sciences. 2019;9(15):2996.

[7] Song S, Dong D, Yan B, Xu F, Huang Y, editors. Natural characteristics for transverse vibration of Euler Bernoulli beams with variable end constraints. Journal of Physics: Conference Series; 2022: IOP Publishing.

[8] Alzghoul M, Cabezas S, Szilágyi A. Dynamic modeling of a simply supported beam with an overhang mass. Pollack Periodica. 2022.

[9] Kudryavtsev IV, Malykhina LK, Morozov SS, Rabetskaya OI, Mityaev AE, editors. Support Coefficients for a Spring-Hinged Beam at Vibration and Buckling2023; Cham: Springer Nature Switzerland.